DEMONSTRATION OF A 600 WATT HYBRID IODINE-XENON ELECTRIC PROPULSION SYSTEM

G.F. Benavides, H. Kamhawi, J.A. Mackey, and T.W. Haag
NASA Glenn Research Center
Cleveland, Ohio

ABSTRACT

This paper reviews iodine-compatible electric propulsion technologies recently evaluated at the NASA Glenn Research Center. The work culminated in a 1,174-hour hybrid iodine-xenon propulsion system durability demonstration (iodine fed thruster with xenon fed cathode). The test demonstrated that (i) a Hall-effect thruster operates with similar performance whether employing iodine or xenon propellant, (ii) careful selection of propulsion system materials and coatings can result in durable iodine-compatible hardware, and (iii) implementation of appropriate facility improvements and procedures can limit negative impacts of iodine on test hardware and ground support equipment. The work was motivated by strong government and commercial interest in the growing capabilities of small-spacecraft (<500 kg), and the remaining desire for denser low-power in-space propulsion to provide small-spacecraft with greater delta-v capability. Volume limitations of small-spacecraft not only require dense propulsion hardware, but more so dense propellants. NASA identifies xenon and iodine as having both favorable storage densities and propulsive properties to enable many NASA small-spacecraft mission scenarios. Xenon is inert and well-proven in spaceflight applications. On the other hand, iodine has triple the storage density of xenon and stores at low pressures, permitting use of conformal tank designs. However, iodine does raise many valid concerns related to its reactivity with most materials, potential spacecraft-propellant interactions, impact on ground test facilities, and challenges to acceptance test iodine propulsion systems prior to flight. As such, the TRL for iodine electric propulsion systems remain low. This work adds to a growing body of research and development efforts aimed at addressing the challenges of utilizing iodine as an electric propulsion propellant. This work was conducted under the Advanced In-Space Propulsion (AISP) project funded through the Game Changing Development (GCD) program within NASA's Science Technology Mission Directorate (STMD).

INTRODUCTION

Since the 1960s, there have been numerous efforts to institutionalize within NASA an exploration and science mission approach of smaller, faster, and cheaper spacecraft[1]. Smaller spacecraft offer NASA many advantages, including reduced development time, lower launch costs, and generally an ability to accept greater risk. Conversely, the drawback of smaller spacecraft is the inability to carry the same diversity of scientific payloads as larger spacecraft. One logical compromise is employing multiple smaller spacecraft with similar, but distributed, capability to a large spacecraft. With multiple smaller spacecraft, loss of any single spacecraft permits continuation of the exploration or science mission, but with only a partial reduction in capability. On the other hand, system failures on a single large spacecraft can effectively end a mission. This is one of many old arguments favoring use of small spacecraft, however recent advances in launch vehicle and spacecraft technologies make now an opportune time to further pursue harnessing small spacecraft for NASA missions. A few recent trends favoring increasing application of small spacecraft for NASA missions include:

1. Many small spacecraft technologies have been increasingly miniaturized and grown in capability in recent years[2], in part driven by the rise of CubeSats;

2. Rideshare opportunities for small spacecraft have rapidly increased, offering frequent low-cost launch opportunities to a wide range of orbits[3]; and

3. U.S. and international aerospace stakeholders are increasing investment in small spacecraft, developing constellations as a lower-cost and lower-risk approach to providing global satellite services[4].

While the appeal of small spacecraft to fulfill needs within the commercial sector grows, challenges persist in the area of highly capable in-space propulsion. In recent years, NASA has applied significant resources towards small- and micro-spacecraft propulsion systems in an attempt to address this need. However, while a handful of the developments are approaching flight readiness, most propulsion developments underway are characteristically more appropriate for commercial LEO applications than long-life deep space missions. This is a natural outcome of commercial industry offering a greater return on investment for businesses pursuing propulsion system developments. Thus, propulsion system developers favor the lower-cost, higher risk tolerant designs favored by LEO small-satellite developers. This is a positive outcome for U.S. commercial spaceflight, however insufficient for NASA exploration and science missions requiring high reliability and very large delta-v propulsive capability. So, even with considerable recent investment in small-satellite propulsion, challenges persist for NASA to identify propulsion technologies that will enable small-spacecraft for NASA missions beyond Earth orbit.

For NASA to pursue deep space exploration and science missions employing small-spacecraft, and benefit from the cost savings associated with rideshare opportunities, small spacecraft on-board propulsion systems must not only have sufficient capability to accommodate non-ideal initial launch trajectories, but also the propulsive capability to escape earth orbit and perform necessary maneuvers en route to their destinations. The state-of-the-art in high specific impulse, high reliability, in-space propulsion is xenon-fed Hall-effect and gridded-ion thrusters. Such thrusters have not only been demonstrated by NASA on the Dawn and Deep Space 1 missions, but they have also been employed throughout commercial spaceflight for decades. Xenon propellant is an inert gas, storable at approximately 1.6 g/cc under pressure, and ionizes easily. The drawbacks of xenon are its high cost and the high storage pressure necessary to achieve 1.6 g/cc. The resultant xenon pressure vessels (>2,000 psi) pose a real and perceived risk to the primary spacecraft offering the rideshare opportunity. Furthermore, since xenon is stored in a high-pressure vessel to achieve the highest attainable storage density, few storage geometries are feasible, limiting packaging options within the tight confines of the small spacecraft. So, while xenon is well proven, and provides considerable performance capability, it still places many limitations on small-spacecraft developers.

In recent years, institutions around the globe, including NASA and the U.S. Air Force have been giving increased attention to iodine as a higher-density, lower-pressure alternative to xenon for highly volume-constrained missions requiring large delta-v propulsive capability. A useful metric by which to understand the benefit of iodine relative to xenon for volume-limited spacecraft is *density-I_{sp}*, where a thruster's specific impulse, I_{sp}, is weighted by the specific gravity of the stored propellant. For a propulsion system with a fixed total impulse requirement, an improvement in *density-I_{sp}* results in a reduction in propulsion system volume requirement. Alternatively, for a fixed propellant storage volume, raising the *density-I_{sp}* of the propulsion hardware increases the delta-v capability of the spacecraft as long as spacecraft mass limitations are not exceeded. Investigations of Hall-effect and gridded-ion thrusters with iodine propellant have consistently demonstrated thruster performance (i.e., specific impulse, thrust, and efficiency) highly similar to performance with xenon[6,7,8]. Thus, given a similar I_{sp} between iodine and xenon propellants, but an ability to store iodine at triple the density of xenon, iodine can, in theory, achieve an *density-I_{sp}* triple that of a propulsion system operated on xenon. In short, if successfully implemented, iodine propellant would offer a significant boost in spacecraft propulsive capability compared the state-of-the-art xenon propellant with potentially no impact on the overall spacecraft size.

2

It is also worth noting that while secondary spacecraft are both volume and mass limited, rideshare mass availability continues to climb. For example, the ESPA ring, originally qualified for a 180 kg capacity per spacecraft, is in the process of being requalified for 300+ kg per spacecraft. Similarly, the ESPA-Grande will be able to accommodate well over 450 kg per spacecraft, rather than its original 300 kg.[9] Thus, while volume allowances for secondary spacecraft will likely remain unchanged in the near future, launch providers are offering greater accommodation to denser secondary payload spacecraft, which in turn favors use of denser spacecraft propellants such as iodine.

On the other hand, while iodine propellant has many advantages for mass and volume constrained systems, there are numerous unique challenges that must first be overcome. Condensable propellants like iodine raise concern of propellant deposition on spacecraft surfaces. Iodine is also highly reactive, creating new and potentially costly development challenges to select appropriate materials for both the propellant feed system and other spacecraft subsystems exposed to the propellant/plume during flight. The iodine feed system also has other unique challenges associated with the low-pressure propellant, such as assuring adequate propellant delivery and fine flow control capability. The feed system and thruster also require greater electrical power to keep wetted surfaces sufficiently heated to avoid iodine deposition and clogging throughout the propulsion system. Furthermore, there are high-temperature iodine material compatibility considerations that apply to both the thruster and cathode. Finally, there are numerous concerns regarding handling of iodine during ground testing (e.g. storage, pumping, health risks, test facility material compatibility, procedures, etc.) and how best to acceptance test iodine fed propulsion systems prior to flight.

This paper will review recent iodine-fed electric propulsion investigations at NASA Glenn Research Center (GRC), which culminated in a 1,174-hour hybrid iodine-xenon propulsion system durability demonstration (iodine fed thruster with xenon fed cathode). Investigations sought to determine iodine compatibility of state-of-the-art (SOA) BaO hollow cathodes, as well as advance feed system and test facility iodine compatibility in preparation for the durability demonstration.

CATHODE INVESTIGATIONS

A Hall-effect thruster requires propellant fed to both the thruster and cathode for operation. While the working fluid fed to the cathode does not necessarily need to be the same gaseous propellant fed to the thruster, only carrying a single propellant is preferable as the simplest solution. Thus, just as a xenon Hall-effect thruster operates with a xenon fed cathode, the ideal configuration for an iodine electric propulsion system would include an iodine-compatible cathode. However, identifying an iodine compatible cathode design has proven very challenging. As such, NASA GRC performed numerous tests of cathode assemblies that used SOA porous tungsten $BaO\text{-}CaO\text{-}Al_2O_3$ impregnated inserts with iodine propellant in advance of the durability demonstration with the goal of identifying a sufficiently appropriate configuration. The cathode assembly and emitter compatibility tests further aimed to determine if a porous tungsten BaO-impregnated emitter could meet the requirements of NASA's Iodine Satellite (iSat)[10] project, which was recently discontinued. Although numerous materials in the cathode assembly demonstrated an acceptable degree of compatibility over the evaluation period, the BaO-impregnated emitters repeatedly failed to meet the longevity and performance requirements for either the durability demonstration or iSat. All cathode standalone tests were performed at NASA GRC's Vacuum Facility 2 (VF2). For this test campaign, VF2 was equipped with both a xenon and iodine feed system. The VF2 iodine and xenon feed system setup allowed rapid transition between the two propellants.

The first test performed (Test #1) incorporated a cathode assembly without the BaO emitter installed. The aim was to investigate the iodine compatibility of cathode assembly materials (except the emitter) at operational temperatures. During Test #1 the cathode assembly orifice plate was instrumented with a thermocouple. The cathode heater current was set to attain

an orifice plate temperature of ~1000 ºC. During Test #1 iodine flow was passed through the cathode tube and orifice. Inspection of the cathode assembly hardware after approximately 24 hours of exposure to iodine at elevated temperature indicated that no component degradation was observable. There was no evidence of iodide formation/deposition or any remnant iodine deposits on the cathode components.

In Test #2, a SOA porous tungsten $BaO-CaO-Al_2O_3$ impregnate emitter was installed inside the cathode tube. As with Test #1, the heater current was set such that an orifice plate temperature of ~1000 ºC was maintained. Similar to Test #1, iodine propellant was injected into the cathode tube. The aim of the test was to establish the emitter's iodine compatibility in the absence of an active plasma. The test duration was approximately 50 hours. Inspection of the cathode assembly after the conclusion of Test #2 indicated:

- Almost complete depletion of the BaO impregnate at the emitter downstream surface (orifice plate end). This outcome results in more difficulty achieving plasma ignition and will eventually lead to cathode end-of-life. Although impregnate depletion occurred, it is worth noting that sufficient impregnate remained, in theory, to allow for electron emission and meet iSat's minimal lifetime requirements. The rate of BaO depletion, however, was deemed too great to support a 1000+ hour durability demonstration;

- Formation of an interesting dendritic structure on the upstream end of the insert was observed; and

- Noticeable and significant deposition of impregnate material on the downstream surface of the cathode orifice plate:

    - Resulting in ~50% reduction of effective cathode orifice diameter (due to deposition in the orifice region); and

    - Impregnate deposition reducing the effective gap between the cathode and keeper plate, which may result in premature voltage breakdown when cathode ignition is attempted.

The third test performed (Test #3a) aimed to demonstrate cathode ignition and current extraction with iodine propellant. Prior to the introduction of iodine, the new cathode assembly was conditioned following NASA GRC standard cathode operating procedures. Initial cathode ignition was performed with xenon and the cathode was operated for ~5 hours to condition the insert surface. Characterization of the cathode assembly with xenon indicated nominal operation with ignition voltage magnitudes of 25V-50V. After establishing a baseline cathode operation with xenon, cathode operation with iodine was attempted and erratic cathode behavior was observed, where the ignition voltage was above 500V and no stable steady-state operation with iodine was achieved. Additionally, after the insert was exposed to iodine, cathode operation when returned to xenon required ignition voltages that were approximately 500V, indicating cathode degradation.

After Test #3a, several changes were incorporated in the same cathode assembly over a series of tests (designated Test #3b-d), which included changes to the anode plate configuration, changes to the cathode-keeper gap, and the addition of "vent holes" on the keeper tube. These changes enabled the attainment of short-term steady-state operation with iodine propellant, but were characterized by inconsistent ignition voltages (frequently >1kV) and unreliable operation. Test #3b-d indicated that operation of a $BaO-CaO-Al_2O_3$ impregnate cathode with iodine working gas leads to accelerated degradation of the cathode. The degradation is indicated by severe etching and porosity of the insert. Test #3d achieved 14 keeper ignition cycles on iodine between 250V and 500V, but stable current extraction could not be achieved. Figure 1a shows a macro-view of a typical insert after operating for <1 hours with iodine. The region shown indicates the severe porosity and rough nature of the insert. In addition to the porosity, a notable depletion of BaO is observed throughout the bulk of the insert. Figure 1b shows a detailed-view of the depleted impregnate. Remaining impregnate within the iodine operated cathode consisted

4

primarily of Al_2O_3 and CaO with depleted levels of BaO, as measured with energy dispersive spectroscopy. The blue ellipse in Figure 1a highlights a region of Ba tungstate formation along the inner emission surface, possibly indicating the mechanism by which Ba is being depleted. Cathode inspection after Test #3c indicated a notable quantity of foreign deposits on both cathode and keeper orifices after operating cathodes on iodine.
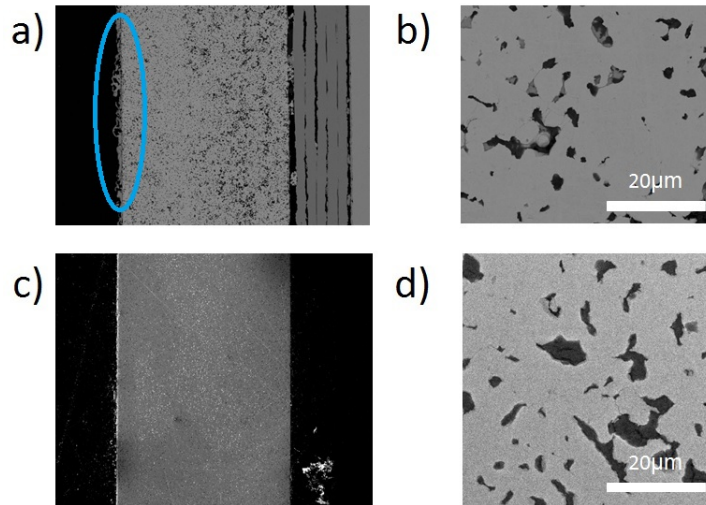
Figure 1: SEM of typical polished cross-sectioned cathode insert. **a)** Macro-view of cathode insert after iodine operation, and **b)** detailed-view of cathode insert after iodine operation. **c)** Macro-view of the insert from a xenon cathode operated with an iodine thruster, and **d)** detailed-view of the insert from a xenon cathode operated with an iodine thruster.

Figure 2a shows a keeper orifice partially obscured with a barium and iodine-containing compound. Likewise deposits of barium containing compounds can be observed in Figure 2c on a cathode orifice plate, Figure 2b is included as a reference image of the orifice plate pre-operation with iodine.
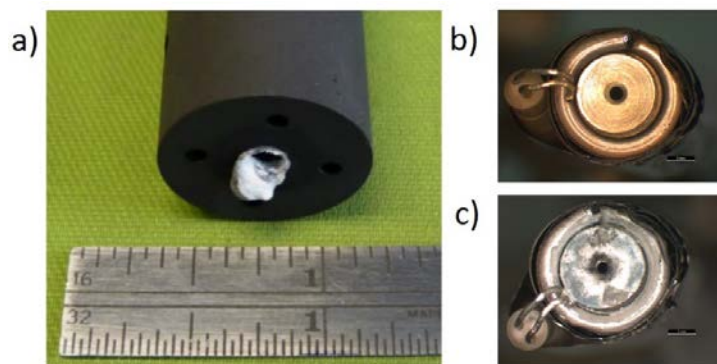
Figure 2: a) Keeper orifice after operating on iodine deposited with barium and iodine containing compound, **b)** cathode orifice before operating on iodine, and **c)** cathode orifice after operating on iodine coated in barium compounds.

As a result of the cathode insert barium depletion by iodine observed during testing, as well as unreliable ignition and steady-state operation with iodine, a cathode based on BaO-CaO-Al_2O_3 impregnate was deemed inadequate to meet iSat requirements. An alternative strategy was investigated for the 1000+ hour durability demonstration, which involved employing a xenon-fed cathode with an iodine-fed thruster. For a flight application, such a hybrid feed system could still achieve a significant reduction in the propellant tank volume compared to an all-xenon

system, since the cathode flow rate is typically on the order of 7% that of the total mass flow. A single propellant for both the thruster and cathode is usually the preferred outcome, but given the many challenges associated with identifying a sufficiently iodine compatible cathode, an iodine thruster with xenon cathode poses the most likely near-term solution that still significantly benefits from iodine's higher density and ability to be packaged in conformal tank designs.

A new cathode assembly was fabricated with a configuration that provides stable cathode operation for extraction currents between 0.5 and 3A. This cathode assembly was used during the 1,174-hour demonstration. After completion of the 1,174-hours demonstration, the insert was removed from the cathode assembly and it was sectioned and analyzed in detail to determine whether any degradation of the insert occurred due to its proximity to the iodine-fed thruster. The cathode insert was not found to be depleted in barium, etched, nor porous, and no iodine was detected within the cathode assembly. Figure 1c and 1d (previous page) show the positive results of a cathode operated for 1,174 hours mostly at a discharge current of 2A with a 0.5A keeper current. No degradation resulting from the close proximity between the xenon-fed cathode and iodine-fed main discharge was detected.   Although an all-iodine system is most desirable to minimize propulsion system complexity, a hybrid iodine-xenon system demonstrates long-term cathode reliability and a compelling near-term solution to increase small spacecraft propulsion system *density-I_{sp}* as research into iodine compatible cathodes is further pursued.

TEST APPARATUS

The thruster implemented in the iodine propulsion system durability test was the Busek BHT-600-I. In the U.S., Busek is arguably leading the development of iodine-compatible electric propulsion technologies[6,7,8]. Busek has demonstrated iodine electric propulsion at numerous power scales with both Hall-effect and gridded-ion thrusters. The BHT-600-I is similar to Busek's BHT-600, but with some alternative materials and coatings to improve iodine compatiblity.

The cathode implemented in the long-duration demonstration was constructed by GRC around a porous tungsten $BaO-CaO-Al_2O_3$ impregnated emitter. As described in the previous section, because of a demonstrated lack of compatibility with iodine propellant, the decision was made to operate the propulsion system as a hybrid. While the thruster had a dedicated iodine storage tank and feed system installed in the vacuum test facility (on the thrust stand), xenon for the cathode was plumbed from an external xenon laboratory feed system. The propulsion system configuration for the long-duration test is illustrated schematically in Figure 3.

An iodine vapor feed system was constructed primarily from 316 stainless steel for the purposes of the demonstration. While 316 SS is not itself highly resistant to corrosion by iodine, it provides a low cost alternative for development testing compared to the high nickel alloys that would most probably be used in construction of a flight iodine propulsion system. To forstall corrosion of the feed system components, the 316 SS was electropolished and coated in silicon[11].

The propellant tank was nominally designed to hold 10 kg of solid iodine propellant with additional volume for ullage. A load of 10 kg would provide upwards of 1200 hours of operation for the BHT-600-I at 300V and 2A. The propellant tank was designed to establish favorable temperature gradients within the iodine storage volume to yield a stable and controllable iodine vapor pressure at the storage tank vapor exit port. The tank thermal gradients were also established to discourage clogging at the vapor exit port. The tank was outfitted with redundant internal cartridge heaters and an external silicon tape heater. Temperatures were monitored at various locations using thermocouples. Iodine flow rate to the thruster was regulated by making adjustments to the power level of the various tank heaters.

A pair of customized solenoid valves as illustrated in Figure 3 were included in the propulsion system assembly. One valve permitted xenon routing to the thruster to establish baseline operation against which iodine operation could be compared. The second valve isolated the iodine tank from the thruster when not in operation or operating with xenon. Both valves were customized at GRC to be iodine resistant and resilient against iodine deposition and clogging.

Wetted materials include silicon coated 316 SS, Teflon™, and viton. The valves include an integral heater cartridge and thermocouple to maintain sufficient temperature to avoid iodine deposition. The valves were actuated using a normally-closed solenoid. The solenoids were operated by a hit-hold methodology to avoid overheating the solenoids during continous operation.
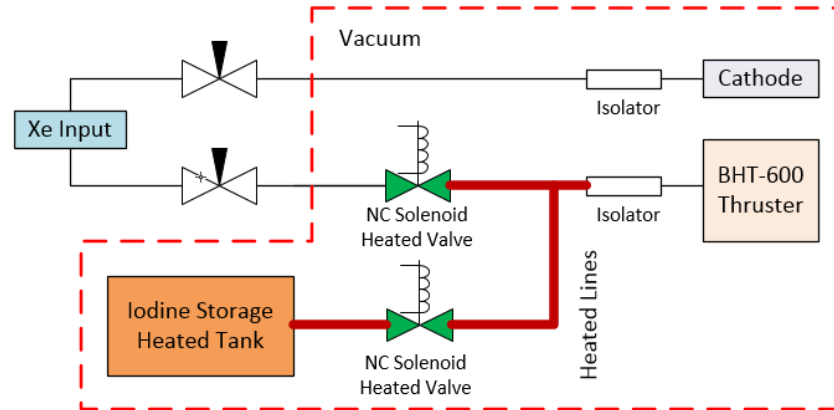
Figure 3: Schematic of iodine propulsion system durability demonstration test setup. Components illustrated inside the dashed line are located inside GRC's Vacuum Facility 7 (VF7) and mounted on the test facility thrust stand.

All tubing between the iodine storage tank and thruster was constructed from nickel alloy C276. Fittings employed throughout the feed system were 316 SS compression fittings as supplied by Swagelok Company. A silicon coating (SilcoTek Silcolloy 1000) was applied to all fittings for added iodine resistance prior to assembly. No pressure measurements were made within the iodine feed system. While pressure data was of interest, inclusion of a pressure sensor was deemed an unnecessary risk and not required for propulsion system operation. Additionally, iodine vapor pressure can be reasonably well predicted based on the iodine storage tank temperature, and iodine flow rate was regulated to provide continuous thruster power by monitoring the discharge current (not a direct iodine flow measurement).
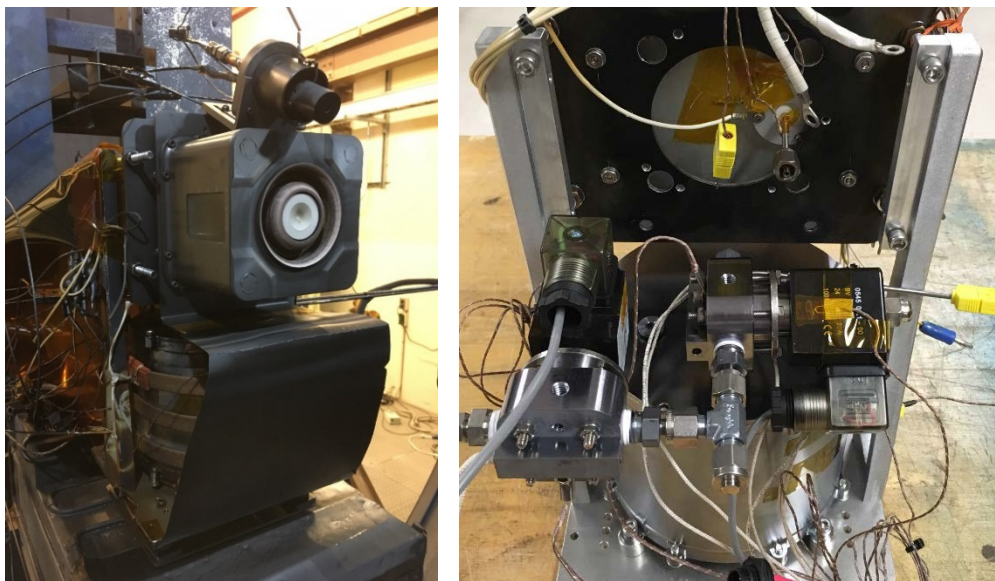
Figure 4: (Left) Iodine propulsion system assembly mounted in GRC Vacuum Facility 7 (VF7). **(Right)** Partially assembled iodine feed system including tank, valves, and fittings.

A photograph of the iodine propulsion system assembly is shown in Figure 4. The GRC xenon fed cathode was mounted at 12 o'clock with respect to the BHT-600-I thruster. The thruster was mounted above and slightly forward of the iodine storage tank to nominally put the propulsion system assembly center of mass directly above the thrust stand. To avoid potential complications related to graphite backsputter from the test facility walls, the propulsion system assembly was strategically protected with grafoil and kapton shields.

VACUUM TEST FACILITY

The iodine electric propulsion system durability demonstration was conducted in Vacuum Facility 7 (VF7) at NASA GRC. VF7 is a 3 meter diameter by 5 meter long vacuum test facility with a 1×10^{-7} torr base pressure (no load). The chamber has five 1m-diameter oil diffusion pumps (ODP) providing a total pumping speed up to 125,000 liters per second at 10^{-6} torr. In preparation for the iodine propulsion system durability demonstration, a number of facility improvements were completed.

Grafoil was applied to the chamber walls downstream of the thruster exit plane. The grafoil provides two primary benefits. First, the backsputter from the chamber walls is reduced during long-duration testing, which results in an accumulation of material on and around the thruster, increasing risk of electrical shorts or other thruster anomalies not consistent with in-space operation. Second, the grafoil slows deterioration of the stainless steel chamber walls resulting from interaction with energetic atomic and molecular iodine. The natural oxide layer formed on the 304 stainless walls in atmosphere provides some corrosion resistance against iodine. However, by allowing the energetic plume to impact directly on the chamber walls, rather than by shielding with a sacrificial material like grafoil, those natural oxides are continuously stripped from the surface, thereby exposing fresh metal and accelerating iodine's corrosive potential.

Similarly, stainless steel threaded studs on the chamber wall were covered with protective graphite nuts that were also used to secure the grafoil in place. Furthermore, immediately above the diffusion pumps, short grafoil tubes were constructed and installed to prevent plume impingement on the walls of the diffusion pump wells and liquid nitrogen cooled chevrons located between the chamber and diffusion pumps. The floor of the chamber was not covered in grafoil to permit ease of access to the chamber and experiment. However, the floor was covered with graphite felt prior to all testing. Ultimately, the graphite felt was deemed a poor choice for floor covering, as the graphite felt was slow to outgas iodine following testing, greatly slowing the decontamination process. While more cumbersome, use of grafoil or graphite plates on the chamber floor for future testing is recommended. The iodine propulsion system assembly as installed in the test facility is shown in Figure 5.

A chilled aluminum target, covered in a single layer of grafoil, was installed in the far end of the chamber as shown in Figure 5. A Polycold heat exchanger, with a cooling capacity capable of achieving -100C, was plumbed to the target to aid in accumulation of iodine during thruster operation. The diffusion pump chevrons were also cooled with liquid nitrogen, providing the primary iodine pumping surface and limiting iodine from entering the oil diffusion pumps. During operation, the liquid nitrogen cooled chevrons provided sufficient pumping capacity to maintain a chamber pressure of approximately 1×10^{-5} torr.

Extraction of the iodine post-test was conducted by sealing the chamber through the use of gate valves, then pumping the iodine toward a Stokes 149 vacuum pump. The liquid-nitrogen cooled chevrons were allowed to warm to room temperature, which results in an iodine vapor pressure of approximately 0.2 torr. A small gas flow of dry-nitrogen was introduced into the chamber to aid in circulation and evacuation of the iodine. To capture the iodine before reaching the Stokes 149, a disposable cold trap was assembled from PVC and polyethylene tubing as shown in Figure 6. A PolyScience 9712 chiller with a temperature capability of -40C circulated a solution of 50/50 water and glycol through the cold trap. A small percentage of the iodine was still

capable of circumventing the cold trap, but was largely collected in the pumps oil, requiring regular pump oil changes following iodine extraction. Following completion of the iodine durability demonstration, the cold trap was sealed and properly disposed.

Figure 5: Iodine propulsion system assembly installed in GRC VF7 prior to 1,174-hour demonstration. All surfaces exposed to direct impingement of the iodine plume are protected with either grafoil, graphite felt, or solid graphite.


Figure 6: (Left) CAD model of the disposable iodine cold trap implemented for the durability demonstration. **(Right)** Photograph of the assembled cold trap chilled using a PolyScience 9712, installed between VF7 and a Stokes 149 vacuum pump.

IODINE PROPULSION SYSTEM DEMONSTRATION RESULTS AND DISCUSSION

In preparation for the long-duration demonstration, the iodine storage tank was loaded with 5,037 grams of iodine on 29 June 2017. Although the iodine tank was designed with the intention of loading 10 kg, equipment necessary to solidify the iodine crystals was not yet available prior to the onset of the demonstration. As a result, loading 99.99+% crystalline iodine

as supplied by Thermo Fisher Scientific Chemicals yielded approximately a 50% packing fraction. A photograph of the iodine tank (a) new and unloaded, (b) loaded with 5 kg crystalline iodine, and (c) after the first 567 hours of testing are shown in Figure 7. At 567 hours, the vacuum facility was decontaminated, the storage tank was refilled with an additional 4,996 grams, and the demonstration was resumed. Note in Figure 7c that no degradation of the silicon-coated storage tank walls was observed. Additionally, thruster operation continued reliably until only the last few grams of iodine shown in Figure 7c remained.
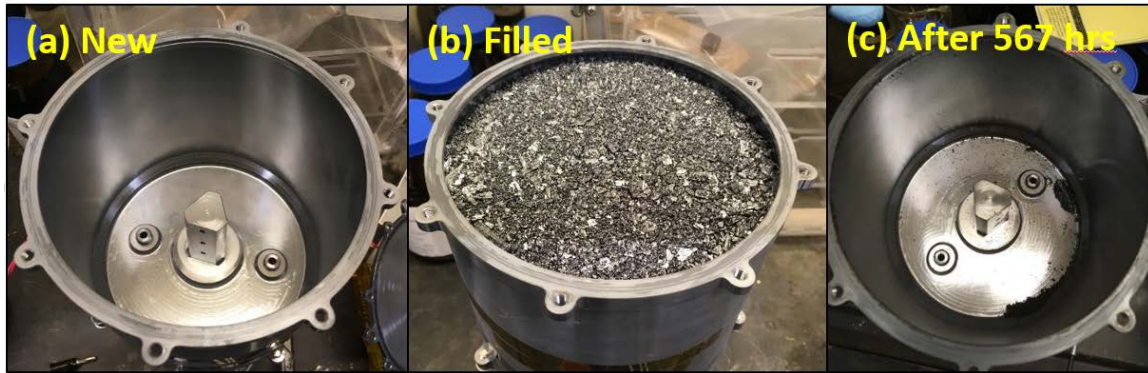
Figure 7: Iodine storage tank used in propulsion system demonstration **(a)** new prior to iodine contamination, **(b)** after first filling with 5kg, and **(c)** after 567 hours of operation.

The iodine demonstration was initiated on 25 July 2017. Prior to flowing iodine, a baseline performance map of the BHT-600-I was established with xenon propellant. At 300V and 2A, with an anode xenon flow rate of 2.52 mg/s and cathode xenon flow rate of 0.2 mg/s, a thrust was measured of 41.3 mN, yielding a specific impulse of 1550 seconds. Similar xenon measurements were made periodically throughout the duration of the iodine demonstration to assess performance against a xenon baseline. Periodic xenon measurements were deemed necessary as no capability was integrated into the test setup to measure instantaneous iodine flow rate, limiting iodine performance assessment to thrust and an average specific impulse. The periodic xenon performance maps are tabulated in Table 1 for various discharge voltages.

Table 1: Thruster xenon periodic performance measurements at 200V, 250V, and 300V.

Xenon Data		200 V				250 V				300 V					
Variable	[Unit]	0 hrs	569 hrs	705 hrs	1,174 hrs	0 hrs	569 hrs	705 hrs	1,174 hrs	0 hrs	307 hrs	*567	**567 hrs	*705 hrs	1,174 hrs
I_d	[A]	2.01	2.20	2.05	2.00	2.01	2.16	2.00	2.01	2.01	2.03	2.05	2.00	2.01	2.01
Xe, Anode	[mg/s]	2.59	2.59	2.40	2.35	2.54	2.54	2.33	2.32	2.52	2.52	2.52	2.41	2.34	2.30
Xe, Cathode	[mg/s]	0.2	0.2	0.2	0.2	0.2	0.2	0.2	0.2	0.2	0.2	0.2	0.2	0.2	0.2
Thrust	[mN]	31.4	29.1	28.1	28.4	37	34.3	31.3	31.7	41.3	39.4	38.2	36.4	35.1	34.8
V_k	[V]	15.0	15.1	15.1	14.9	14.0	16	15.3	15.0	14.3	14.7	14.8	15.0	15.2	14.9
V_{c-g}	[V]	-15.7	-13.5	-13.9	-13.4	-16.1	-14.6	-13.2	-13.1	-16.1	-14.2	-14.0	-14.1	-13.7	-13.5
I_d P-P	[A]	2.48	3.92	2.56	2.00	2.52	4.32	3.28	4.48	2.68	3.00	1.20	4.44	4.00	3.36
I_d RMS	[A]	2.10	2.35	2.10	2.26	2.12	2.33	1.92	2.36	2.13	2.17	2.26	2.27	2.24	2.08
Isp	[s]	1147	1063	1102	1135	1377	1276	1261	1282	1548	1477	1432	1422	1409	1419
Thrust/Pwr	[mN/kW]	78.1	66.1	68.5	71.0	73.6	63.5	62.6	63.1	68.5	64.7	62.1	60.7	58.2	57.7

*Before Event, **After Event

Following establishment of the xenon performance baseline, the cathode was maintained at 0.2 mg/s xenon and the iodine tank temperature was slowly raised until a discharge current of 2A was achieved at 300V. The storage tank temperature was slowly adjusted over the duration of the demonstration as required to maintain a discharge current of 2A at 300V. Discharge current was nearly always maintained between 1.97 and 2.03 amps over the duration of the demonstration with only slight manual temperature adjustments every 8-12 hours. Finer discharge current control could have been achieved by instituting a closed-loop control, but man-

in-the-loop was deemed most appropriate for this demonstration given initial uncertainties regarding the systems operational characteristics. For comparison, select performance data on iodine taken at times similar to the xenon performance map is presented in Table 2. Iodine mass flow rate is estimated based on the average iodine exhausted for each tank load. The iodine mass flow rate at 540 hours is estimated as the average over the entire 1174-hour test. As such, the specific impulses presented in Table 2 are only estimates. However, the thrust and specific impulse for both iodine and xenon track well throughout the demonstration.

Table 2: Thruster iodine performance measurements at 300V. Iodine mass flow rate and specific impulse estimated based on average iodine exhausted over the demonstration.

Iodine Data		300 V						
Variable	[Unit]	1 hrs	308 hrs	*540 hrs	**569	*705 hrs	**705	1,144 hrs
I_d	[A]	2.06	2.02	1.98	1.94	1.99	2.00	2.00
I_2, Estimate	[mg/s]	2.47		2.38			2.29	
Xe, Cathode	[mg/s]	0.2	0.2	0.2	0.2	0.2	0.2	0.2
Thrust	[mN]	40.7	38.2	34.7	33.9	34	34.6	33.5
V_k	[V]	14	13.9	14.6	15.2	14.6	15.0	15.1
V_{c-g}	[V]	-16.8	-14.8	-14.0	-14.3	-14.1	-14.6	-14.4
I_d P-P	[A]	1.6	2.60	1.2	2.96	2.80	1.82	2.56
I_d RMS	[A]	2.09	2.25	2.11	2.16	2.16	2.09	2.00
Isp, Estimate	[s]	1554	1458	1371	1339	1392	1416	1371
Thrust/Pwr	[mN/kW]	65.9	63.0	58.4	58.2	57.0	57.7	55.8

*Before Event, **After Event

Figure 8 is a photograph of the BHT-600-I operating at 300V, 2A on iodine in GRC VF7 at approximately 600-hours. For a more thorough comparison of the BHT-600-I on both iodine and xenon throughout the demonstration, the thrust-to-power ratio (mN/kW) is plotted in Figure 9. Again note that iodine and xenon performance tracked well throughout the demonstration, each showing an approximate 16% reduction in thrust-to-power over 1174-hours. The test demonstrates that from a purely performance perspective iodine is nearly a one-to-one replacement for xenon in Hall-effect thrusters.
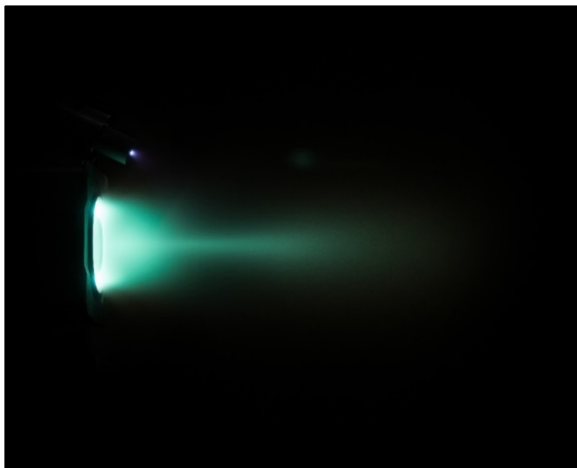
Figure 8: BHT-600-I operating on iodine matched with a GRC cathode operating on xenon in GRC VF7.
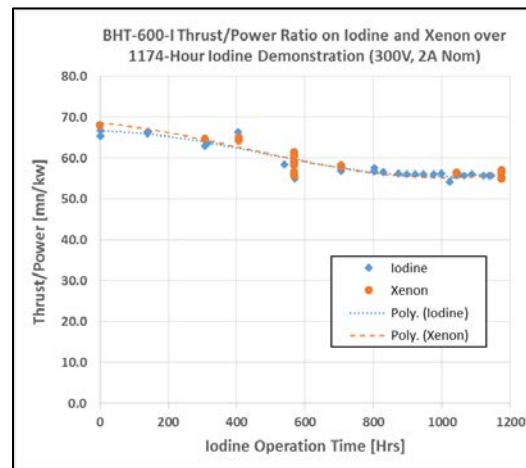
Figure 9: BHT-600-I thrust to power ratio for iodine and xenon over 1174-hour iodine demo.

Although the overall demonstration of an iodine electric propulsion system was quite successful, there were a number of challenges throughout the 1174-hour test. A timeline of events is provided in Table 3. Most notably, on 21 August 2017 an uncontrolled purge of iodine from VF7 occurred. Following a liquid nitrogen (LN2) delivery, a vent valve was not properly resealed by the contractor resulting in an eventual loss of the LN2 tank pressure. Without

sufficient tank head pressure, LN2 ceased being delivered to VF7, resulting in a loss of iodine containment on the LN2 chevrons. Heat from the ODPs sublimated the iodine, which exhausted into the primary roughing train, became trapped in the roughing pump oil, and in part vented to the facility roof. While the LN2 system failure did not endanger the experiment or personnel, significant vacuum facility iodine contamination occurred, requiring approximately one month to remediate before testing could resume. Should future iodine work be performed in VF7, facility modifications are recommended to prevent such a future occurrence.

Also, on 2 October 2017, the propulsion system ceased functioning while operating on iodine. An attempt to restart the propulsion system on xenon was unsuccessful. The propulsion system was behaving in a manner characteristic with an electrical short. The chamber was decontaminated and vented to access the experiment and assess the issue. It was determined that a non-iodine compatible ring-terminal internal to the BHT-600-I was employed to attach the anode power line during thruster assembly. The failure of such a minor component illustrates the vigilance that will be required for production of highly reliable iodine resistant spaceflight hardware. The thruster manufacturer was consulted, a repair plan was developed, and the ring-terminal was successfully replaced without removing the propulsion system from the test stand.

While repairing the anode power ring-terminal, physical inspection of the test article noted that alloying elements were being leached from the thruster body, most specifically thruster body internal surfaces exposed to high temperature during thruster operation. The issue did not present a complication during the thruster demonstration, but selection of alternate materials for these components are recommended for future iodine-compatible thruster iterations.

Table 3: Timeline of events for 1174-hour iodine propulsion demonstration.

#	Date	Event	I$_2$ Hrs	Comments
1	06/29/17	Load iodine	---	5.037 kg iodine loaded
2	07/25/17	Demonstration initiated	0	Baseline on xenon; initiated iodine demonstration
3	08/07/17	Thrust stand calibration	307	Assess performance with xenon at 300V
4	08/11/17	Discharge over-current	405	Auto-shutdown; Cause unknown; Assess performance xenon
5	08/17/17	Thrust stand calibration	540	
6	08/18/17	Thruster shutdown	567	Iodine exhausted
7	08/21/17	Thruster checkout	567	Assess performance with xenon
8	08/21/17	LN2 failure	567	Uncontrolled vent of iodine
9	09/01/17	Thruster checkout	567	Assess performance with xenon
10	09/07/17	Vent chamber	567	Vent and decontaminate to access experiment
11	09/20/17	Load iodine	567	4.996 kg iodine loaded
12	09/25/17	Thruster checkout	567	Assess performance with xenon
13	09/26/17	Demonstration resumed	567	Checkout on xenon; resumed iodine demonstration
14	10/02/17	Discharge over-current	705	Auto-shutdown; Unable to restart
15	10/03/17	Vent chamber	705	Vent and decontaminate to access experiment
16	10/18/17	Diagnose thruster	705	Anode power line failed at anode termination
17	10/23/17	Repair	705	Replaced anode power line termination
18	10/30/17	Demonstration resumed	705	Checkout on xenon; resumed iodine demonstration
19	11/03/17	Thrust stand calibration	802	Calibrate thrust stand; resumed iodine demonstration
20	11/13/17	Thrust stand calibration	1044	Calibrate thrust stand; resumed iodine demonstration
21	11/18/17	Thruster shutdown	1174	Iodine exhausted; Auto-shutdown
22	11/20/17	Thrust stand calibration	1174	Assess performance with xenon

The demonstration was completed on 18 November 2017 when the second load of iodine was exhausted. Up until the last of the iodine was exhausted, operation of the propulsion system was stable and reliable. The primary goal to demonstrate greater than 1,000-hours of propulsion system operation on iodine was achieved, although a fill operation and minor repair operation were required. While there was no attempt made to collect data necessary to estimate the lifetime of the propulsion system on iodine, no difficulties existed at the conclusion of the test that would have prevented further testing had it been decided to continue.

Figures 10 through 11 below present the power spectral density (PSD) profiles for the BHT-600-I discharge current waveforms for xenon and iodine operation, respectively, at a discharge current of ~2A at selected test durations. Profiles presented in Figure 10 indicate that there was a shift in the discharge dominnat frequency from ~35 khz to ~43 khZ after operating for ~307 hours. The PSD profile at 567 hour (prior to end of Segment 1) indicates another change in the PSD profile that indicates a change in the thruster's discharge characteristics (Table 1 shows a change in the Pk2Pk from 3 A at 307 hours to 4.44 A at 567 hours). The change in the profile may be attributed to changes in the discharge channel profile due to erosion and due to the degradation of the dielectric coating on the thruster's midstem which could be causing a change in the current collected by the thruster. The test was then halted to reload iodine. After restarting the test, the measured PSD profile indicates a profile that is different than prior to halting the test, this could be attributed to the fact that the facility background pressure was higher during the second test segment. The PSD profiles at 567, 705, and 1,174 hours are very similar; it is speculated that the slight change in the discharge current wavefore may be an indication that the discharge channel profile might have progressed to a profile that is close to its EOL and as such no significant changes in the discharge waveform were further occuring.
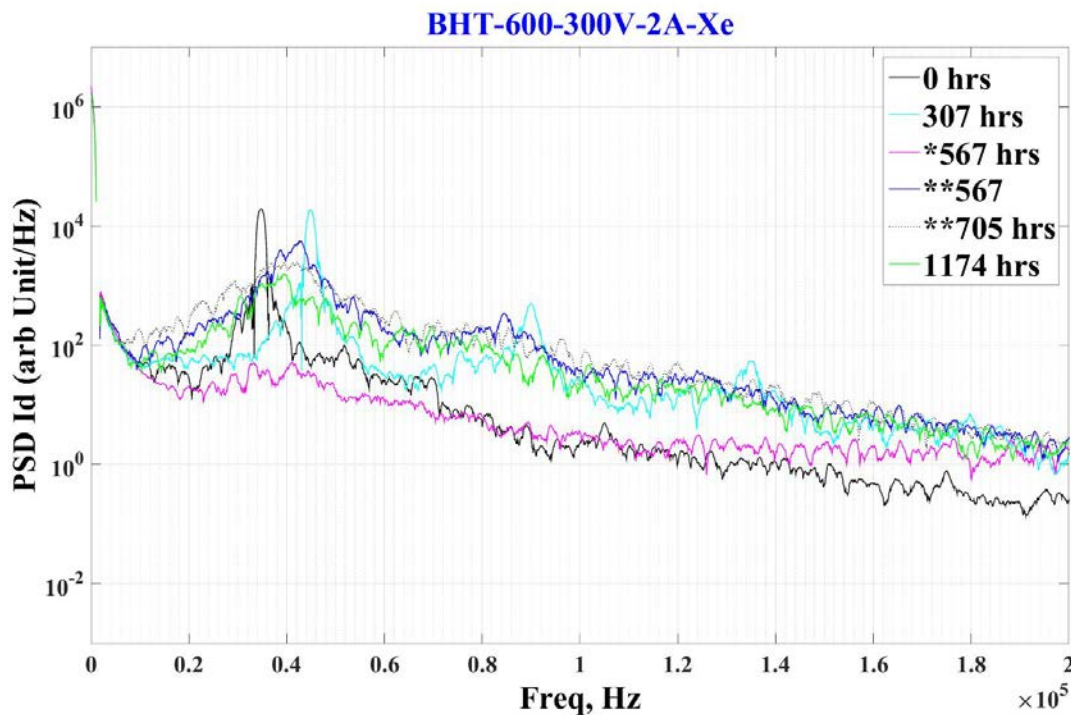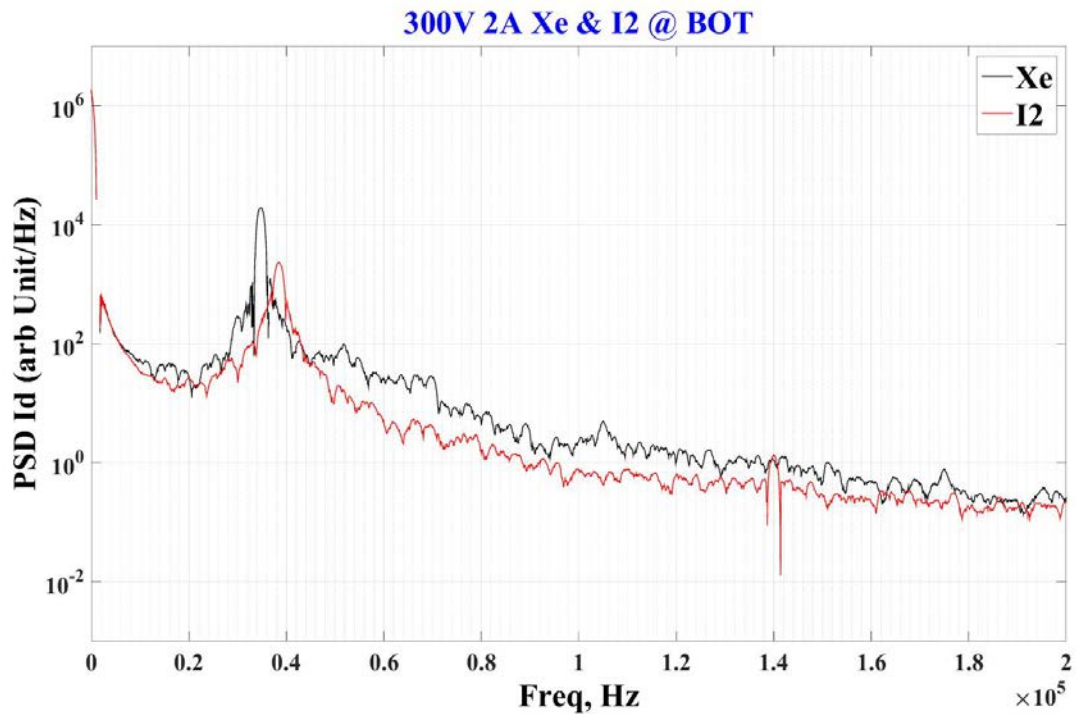

Figure 10: BHT-600-I discharge current waveform PSDs for xenon propellant operation.

Figure 11 presents the discharge current PSDs for iodine propellant operation. The trends presented in Figure 11 are very similar to the ones presented in Figure 10. In segment 1

noticeable changes occurred in the discharge current waveform profiles (dominant frequency, Pk2Pk, and RMS) but in segment 2 the changes were much less noticable.
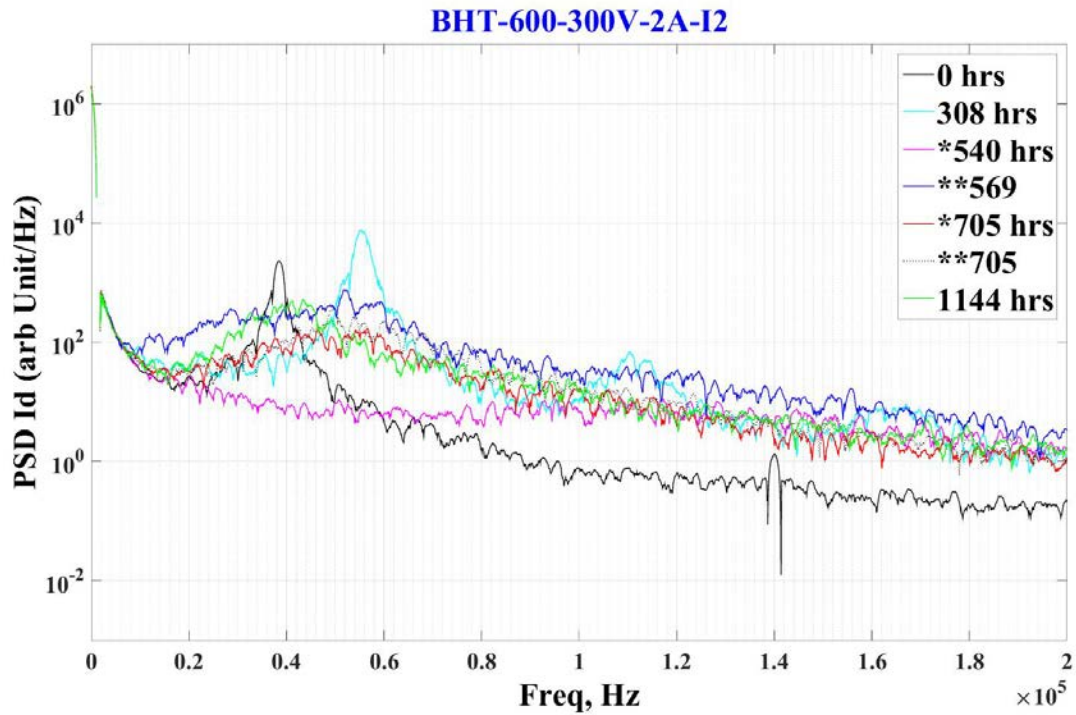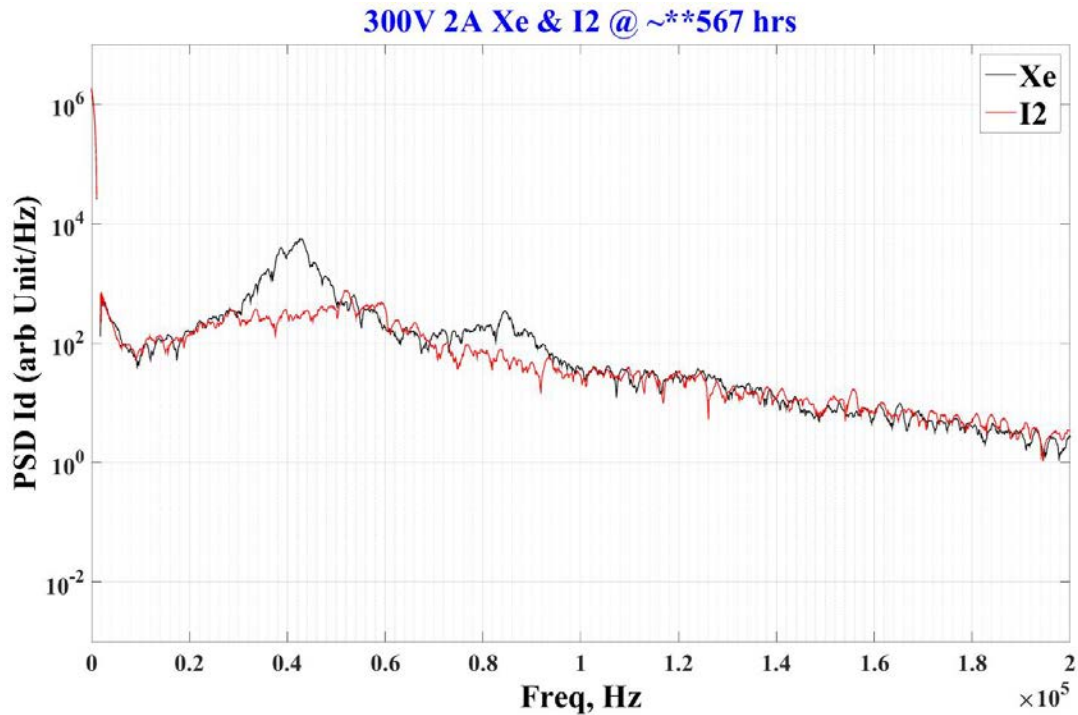

Figure 11: BHT-600-I discharge current waveform PSDs for iodine propellant operation.
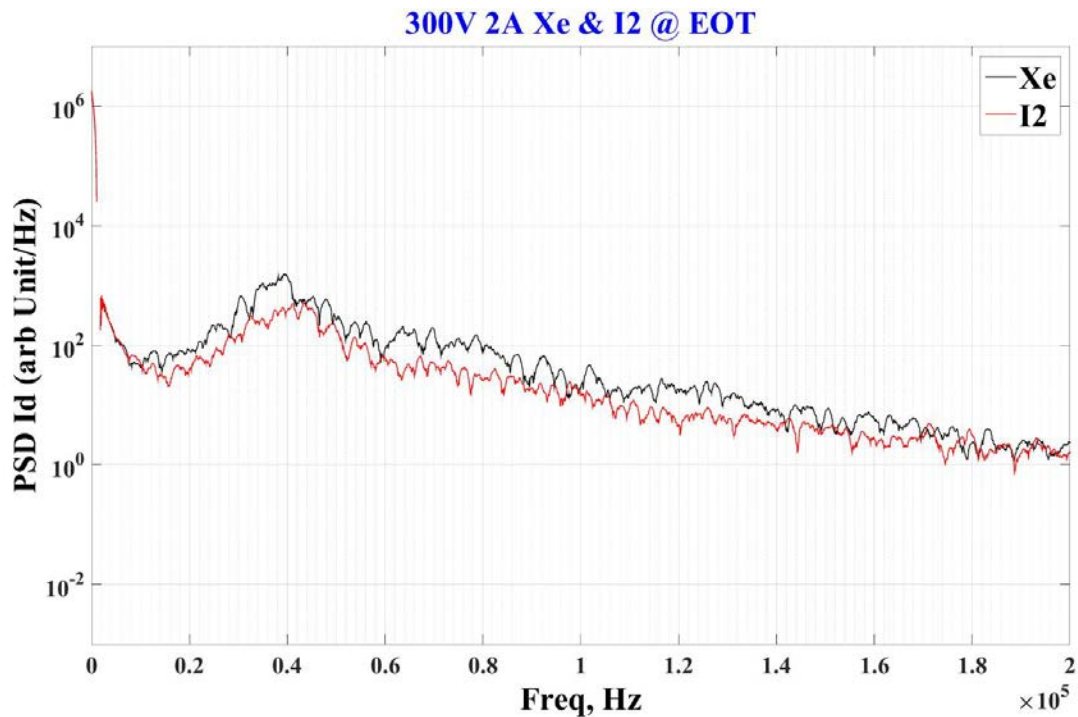

Figure 12: BHT-600-I discharge current waveform PSDs for xenon and iodine at BOT.

Figures 12, 13, and 14 present a comparison between discharge current PSDs for xenon and iodine operation at beginning of test (BOT), 567, and end of test (EOT), respectively. The Figures indicate that, in general, the discharge current Pk2Pk is lower for iodine operation when compared to xenon, and that the variation of the PSD profiles with time is similar for xenon and iodine propellants.

Figure 13: BHT-600-I discharge current waveform PSDs for xenon and iodine at 550 hours.

Figure 14: BHT-600-I discharge current waveform PSDs for xenon and iodine at 1,174 hours.

SUMMARY AND CONCLUSIONS

This paper reviewed recent iodine compatible electric propulsion technologies evaluated at the NASA Glenn Research Center. The work culminated in a 1,174-hour hybrid iodine-xenon propulsion system durability demonstration (iodine fed thruster with xenon fed cathode). The demonstration employed a Busek BHT-600-I Hall-effect thruster, a GRC BaO hollow cathode, and a GRC iodine feed system. The propulsion system was operated using laboratory power supplies. While the initial intent was to operate the propulsion system all-iodine to minimize system complexity, a sufficiently iodine compatible cathode could not be identified, and as a result the system was operated in a hybrid iodine-xenon configuration. For a flight application, a hybrid feed system would still achieve a significant reduction in the propellant tank volume compared to an all-xenon system, since the cathode flow rate is typically on the order of 7% that of the total propellant mass flow, but avoid the known iodine-compatible cathode development challenges. The test demonstrated:

    (i)   a Hall effect thruster operates with similar performance whether employing iodine or xenon propellant over long-duration;

    (ii)   careful selection of propulsion system materials and coatings can result in durable iodine-compatible hardware; and

    (iii)   implementation of appropriate facility improvements and procedures can limit negative impacts of iodine on test hardware and ground support equipment.

Although some inadequacies of the experimental hardware and test facilities were revealed through a loss of iodine containment at 567-hours and an electrical connection failure at 705-hours, demonstration of 1,174 total hours of operation verify that implementation of iodine as a propellant in electric propulsion devices is feasible, although challenging. A lack of contamination or degradation of the xenon-fed cathode assembly in proximity to the iodine-fed thruster is also encouraging as an interim solution until sufficiently iodine compatible cathodes are developed. Use of coating such as silicon, as demonstrated in the laboratory iodine feed system, may also provide direction for low-cost methods to improve iodine compatibility of spacecraft subsystems. Nonetheless, as encouraging as the demonstrations results, it is also clear that much work remains in further refining iodine propulsion system technologies, constructing dedicated iodine compatible test facilities, and better understanding the potential long-term impacts of iodine plumes on spacecraft systems and payloads.

ACKNOWLEDGMENTS

REFERENCES

1. Roy, S. A., ***The origin of the smaller, faster, cheaper approach in NASA's solar system exploration program***, Space Policy, volume 14, issue 3, 1998, p152-171.
2. **Small Spacecraft Technology State of the Art**, Mission Design Division, Ames Research Center, Moffett Field, CA, 2015
3. Karuntzos, K., **United Launch Alliance Rideshare Capabilities for Providing Low-Cost Access to Space**, IEEE, Big Sky, MT, 2015.

4. Alvarez, J., **Constellations, Clusters, and Communication Technology: Expanding Small Satellite Access to Space**, IEEE, Big Sky, MT, 2016.
5. Maly, J. R. and Stender, M., **Moog Capabilities for Small Satellites,** 13th Annual CubeSat Developer's Workshop, San Luis Obispo, CA, 2016.
6. Szabo, J., Pote, B., Paintal, S., Robin, M., Kolencik, G, Hillier, A., Branam, R. D., and Huffman, R. E., Performance Evaluation of an Iodine Vapor Hall Thruster, 47th AIAA/ASME/SAE/ASEE Joint Propulsion Conference, San Diego, CA, 2011.
7. Szabo, J., Robin, M., Paintal, S., Pote, B., Hruby, V., and Freeman, C., **Iodine Propellant Space Propulsion**, International Electric Propulsion Conference, Washington D.C., 2013.
8. Tsay, M., Frongillo, J., Model, J., Zwahlen, J., and Paritsky, L., **Maturation of Iodine-Fueled BIT-3 RF Ion Thruster and RF Neutralizer**, 52nd AIAA/SAE/ASEE Joint Propulsion Conference, Salt Lake City, UT, 2016.
9. Maly, J. R., Sandord, G. E., Williams, A., and Berenberg, L., **ESPA Class Redefined**, 31st Annual AIAA/USU Conference on Small Satellites, Logan, UT, 2017.
10. Jehle, A., **Iodine Small Satellite Propulsion Demonstration – iSAT**, 31st AIAA/USU Conference on Small satellites, Logan, UT, 2017.
11. Costa, G.C., Benavides, G.F., and Smith, T.D., **Chemical, Structural, and Microstructural Changes in Metallic and Silicon-Based Coating Materials Exposed to Iodine Vapor**, NASA/TM-2017-219498.